J|A|C|S
ARTICLES
Published on Web 06/13/2006

Demonstrating Oxygen Loss and Associated Structural Reorganization in the Lithium Battery Cathode $Li[Ni_{0.2}Li_{0.2}Mn_{0.6}]O_2$

A. Robert Armstrong,[†] Michael Holzapfel,[‡] Petr Novák,[‡] Christopher S. Johnson,[§] Sun-Ho Kang,[§] Michael M. Thackeray,[§] and Peter G. Bruce*,[†]

Contribution from EaStCHEM, School of Chemistry, University of St Andrews, St. Andrews, Fife, KY16 9ST, United Kingdom, Paul Scherrer Institut, 5232 Villigen PSI, Switzerland, and Chemical Engineering Division, Argonne National Laboratory, Argonne, Illinois 60439, U.S.A.

Received March 24, 2006; E-mail: p.g.bruce@st-andrews.ac.uk

Abstract: The cathode in rechargeable lithium-ion batteries operates by conventional intercalation; Li^+ is extracted from $LiCoO_2$ on charging accompanied by oxidation of Co^{3+} to Co^{4+}; the process is reversed on discharge. In contrast, Li^+ may be extracted from Mn^{4+}-based solids, e.g., Li_2MnO_3, without oxidation of Mn^{4+}. A mechanism involving simultaneous Li and O removal is often proposed. Here, we demonstrate directly, by in situ differential electrochemical mass spectrometry (DEMS), that O_2 is evolved from such Mn^{4+}-containing compounds, $Li[Ni_{0.2}Li_{0.2}Mn_{0.6}]O_2$, on charging and using powder neutron diffraction show that O loss from the surface is accompanied by diffusion of transition metal ions from surface to bulk where they occupy vacancies created by Li removal. The composition of the compound moves toward MO_2. Understanding such unconventional Li extraction is important because Li−Mn−Ni−O compounds, irrespective of whether they contain Co, can, after O loss, store 200 $mAhg^{-1}$ of charge compared with 140 $mAhg^{-1}$ for $LiCoO_2$.

Introduction

Rechargeable lithium-ion batteries are the most important development in portable energy storage for 100 years. They have a vital role to play in combating global warming (hybrid electric vehicles), powering implantable medical devices (artificial heart), and a myriad of other applications. The cathode in rechargeable lithium-ion batteries, usually $LiCoO_2$, functions by Li^+ extraction/insertion on charge/discharge, associated with oxidation/reduction of the transition metal ion, Co in the case of $LiCoO_2$, i.e., by conventional lithium intercalation.[1−4] However, for a number of years it has been known that lithium may be extracted from lithium manganese-based oxides, such as Li_2MnO_3, containing Mn^{4+} ions, without oxidation of the transition metal ion.[5−8] This phenomenon has been observed in many manganese-based oxides.[9−19] Clearly, the process is not simply deintercalation; how, then, can such a process be explained? In some cases, lithium extraction is accompanied by oxidation of the nonaqueous electrolyte (e.g., $LiPF_6$ in ethylene carbonate/dimethyl carbonate), generating H^+ ions that exchange with Li^+.[6−8,10−12] This is also the dominant mechanism for oxidation by aqueous acid and NO_2BF_4 in acetonitrile.[6,12] However, in other instances, H^+ ion exchange cannot explain the process. In these cases, an alternative mechanism involving the simultaneous removal of Li and O from the solid has been invoked.[9,10,13−15] It is important to understand this process in its own right but also because following such unconventional Li extraction from lithium−manganese−nickel−oxides, irrespective of whether they contain cobalt, the materials can deliver reversible capacities of 200 $mAhg^{-1}$, compared with 140$mAhg^{-1}$ for $LiCoO_2$.[20−26] Such capacities represent a

[†] EaStCHEM, School of Chemistry, UK.
[‡] Paul Scherrer Institut.
[§] Argonne National Laboratory.

(1) Tarascon, J.-M.; Armand, M. *Nature* **2001**, *414*, 359.
(2) Aricò, A. S.; Bruce, P. G.; Scrosati, B.; Tarascon, J.-M.; van Schalkwijk, W. *Nature Mater.* **2005**, *4*, 366.
(3) van Schalkwijk, W. A., Scrosati, B., Eds. *Advances in Lithium-Ion Batteries*; Kluwer Academic/Plenum Publishers: New York, 2002.
(4) Nazri, G.-A., Pistoia, G., Eds. *Lithium Batteries Science and Technology*; Kluwer Academic Publishers: Boston, 2004.
(5) Kalyani, P.; Chitra, S.; Mohan, T.; Gopukumar, S. *J. Power Sources* **1999**, *80*, 103.
(6) Rossouw, M. H.; Thackeray, M. M. *Mater. Res. Bull.* **1991**, *26*, 463.
(7) Robertson, A. D.; Bruce, P. G. *Chem. Commun.* **2002**, 2790.
(8) Robertson, A. D.; Bruce, P. G. *Chem. Mater.* **2003**, *15*, 1984.
(9) Lu, Z.; Dahn, J. R. *J. Electrochem. Soc.* **2002**, *149*, A815.
(10) Armstrong, A. R.; Bruce, P. G. *Electrochem. Solid-State Lett.* **2004**, *7*, A1.
(11) Ammundsen, B.; Jones, D. J.; Rozière, J.; Burns, G. R. *Chem. Mater.* **1995**, *7*, 2151.
(12) Venkatraman, S.; Manthiram, A. *J. Solid State Chem.* **2004**, *177*, 4244.
(13) Robertson, A. D.; Bruce, P. G. *Electrochem. Solid-State Lett.* **2004**, *7*, A294.
(14) Armstrong, A. R.; Bruce, P. G. *J. Mater. Chem.* **2005**, *15*, 218
(15) Armstrong, A. R.; Robertson, A. D.; Bruce, P. G. *J. Power Sources* **2005**, *146*, 275.
(16) Sun, Y.-K.; Kim, M.-G.; Kang, S.-H.; Amine, K. *J. Mater. Chem.* **2003**, *13*, 319.
(17) Kang, S.-H.; Sun, Y.-K.; Amine, K. *Electrochem. Solid-State Lett.* **2003**, *6*, A183.
(18) Grey, C. P.; Yoon, W.-S.; Reed, J.; Ceder, G. *Electrochem. Solid-State Lett.* **2004**, *7*, A290.
(19) Yoon, W.-S.; Kim, N.; Yang, X.-Q.; McBreen, J.; Grey, C. P. *J. Power Sources* **2003**, *119*−*121*, 649.
(20) Spahr, M. E.; Novak, P.; Schnyder, B.; Haas, O.; Nesper, R. *J. Electrochem. Soc.* **1998**, *145*, 1113.
(21) Ohzuku, T.; Makimura, Y. *Chem. Lett.* **2001**, *8*, 744.
(22) Lu, Z.; MacNeil, D. D.; Dahn, J. R. *Electrochem. Solid-State Lett.* **2001**, *4*, A191.
(23) Lu, Z.; Beaulieu, L. Y.; Donaberger, R. A.; Thomas, C. L.; Dahn, J. R. *J. Electrochem. Soc.* **2002**, *149*, A778.
(24) Johnson, C. S.; Kim, J−S.; Lefief, C.; Li, N.; Vaughey, J. T.; Thackeray, M. M. *Electrochem. Commun.* **2004**, *6*, 1085.

10.1021/ja062027+ CCC: $33.50

significant step forward in energy storage compared with the traditional materials.[26] Despite the important role of this activation process in accessing higher levels of energy storage, direct proof of oxygen loss and the detailed process of structural reorganization have not been given. Here we demonstrate directly, by in situ electrochemical mass spectroscopy, that oxygen is lost from such compounds and, by neutron diffraction which is more sensitive to the location of Li than X-rays, the details of how this is achieved by structural rearrangement.

Of particular importance is the electrode system $Li[Ni_x Li_{1/3-2x/3}Mn_{2/3-x/3}]O_2$ ($0 \le x \le 0.5$), in which three Ni^{2+} ions substitute for two Li^+ ions and one Mn^{4+} ion in the layered compound Li_2MnO_3 ($Li[Li_{1/3}Mn_{2/3}]O_2$).[9,22,23] Several groups have demonstrated that following lithium deintercalation and the associated oxidation of Ni^{2+} to Ni^{4+}, lithium may continue to be extracted from this material despite the fact that all the manganese and nickel ions are in their fully charged (+4) oxidation state.[9,13,15−18] This process is associated with a well-defined plateau at 4.5 V, at which potential there is little or no evidence of H^+-ion exchange. For these reasons, and because such materials form the basis of cathodes that can deliver capacities in excess of 200 $mAhg^{-1}$, following activation by charging across the 4.5 V plateau, we have chosen a composition in this system to investigate the phenomenon further.

Experimental Section

Synthesis. $Li[Ni_{0.2}Li_{0.2}Mn_{0.6}]O_2$ was synthesized from mixed nickel−manganese carbonate and lithium carbonate precursors by a coprecipitation method. First, a 0.2 M aqueous solution of nickel sulfate and manganese sulfate (Ni/Mn = 1:3) was added to a 1 M, equivolume, aqueous solution of sodium hydrogen carbonate, from which green precipitates formed instantly; the mixed solution was aged for 24 h. The coprecipitation and aging procedures were carried out under constant stirring (250 rpm) at 50 °C. The $(Ni_{0.25}Mn_{0.75})CO_3$ precipitate was filtered, washed, dried at 108 °C, and thereafter intimately mixed with Li_2CO_3. The $Li[Ni_{0.2}Li_{0.2}Mn_{0.6}]O_2$ product was obtained by firing the mixed precursors at 900 °C for 6 h in air.

Samples for neutron diffraction were prepared electrochemically using Swagelock cells. The working electrodes consisted of 85 wt % active material and 15 wt % Super S carbon with no binder. The active material and Super S were ground together and then loaded into the cell. A Li metal counter electrode was used with a 1 mol solution of $LiPF_6$ in EC/DMC (1:1 V/V, Merck) as electrolyte. Cells were charged at a rate of 10 mAg^{-1} at 30 °C to the appropriate cutoff potential using a Biologic Macpile II. After charging, cells were transferred to an argon-filled glovebox before opening, and the active material was removed. The electrodes were then rinsed with a small amount of dry solvent (DMC) to remove residual electrolyte. They were then left under dynamic vacuum overnight to ensure all solvent had evaporated. The samples were then transferred to 2 mm quartz capillaries.

The structures of the materials were characterized using neutron diffraction. Time-of-flight powder neutron diffraction data were collected on the GEM high-intensity, medium-resolution instrument at ISIS, Rutherford Appleton Laboratory. The structures were refined by the Rietveld method using the program Prodd based on the Cambridge Crystallographic Subroutine Library (CCSL).[27] Neutron scattering lengths of −0.19, −0.373, 1.03, and 0.5803 (all $\times 10^{-12}$ cm) were assigned to Li, Mn, Ni, and O, respectively.[28]

In situ differential electrochemical mass spectrometry (DEMS) analysis was carried out to detect the gases generated during charging. The cell consisted of a lithium anode, electrolyte (1 mol solution of $LiPF_6$ in EC/DEC (1:2 V/V, Merck)), and the working positive electrode. The latter was formed by casting a mixture of the active material, Super S carbon, and Kynar Flex 2801 binder in NMP in the weight ratios 80:10:10 on the titanium current collector and drying at 120 °C overnight. The cell was purged continuously with Ar gas, which flowed from the cell into the mass spectrometer carrying the evolved gases for MS analysis. The experimental setup is described in detailed elsewhere.[29] The cell potential was raised in 100 mV steps from 4.3 to 4.8 V every 120 min with a sweep rate of 0.1 mV/s and the variation of the ion current for different m/z (mass per electron) monitored as a function of time.

Results and Discussion

Detailed high-resolution transmission electron microscopy (HRTEM), nuclear magnetic resonance (NMR), and computational studies, carried out previously, revealed that the structures of $Li[Ni_xLi_{1/3-2x/3}Mn_{2/3-x/3}]O_2$ electrode materials are highly complex;[25,30] they are characterized by short-range order of the cations extending to microphase separation. As such, they can be described as having nanocomposite structures derived from a pseudo binary $xLiNi_{0.5}Mn_{0.5}O_2 \cdot (1-x)Li_2MnO_3$ system with $LiNi_{0.5}Mn_{0.5}O_2$ and Li_2MnO_3 end members, rather than a solid solution.[22] It has, of course, been known since the pioneering work on the Wadsley-Roth phases that true solid solutions are rare on the nanoscale.[31] We selected an electrode composition $0.5LiNi_{0.5}Mn_{0.5}O_2 \cdot 0.5Li_2MnO_3$, corresponding to $x = 0.2$ in $Li[Ni_xLi_{1/3-2x/3}Mn_{2/3-x/3}]O_2$, i.e., $Li[Ni_{0.2}Li_{0.2}Mn_{0.6}]O_2$, which provides substantial capacity during an initial charge at 4.5 V. In the discussion that follows, we use $Li[Ni_{0.2}Li_{0.2}Mn_{0.6}]O_2$ for convenience to define the composition of our electrode.

In a general sense, $Li[Ni_xLi_{1/3-2x/3}Mn_{2/3-x/3}]O_2$ compounds have a layered α-$NaFeO_2$-type structure ($R\bar{3}m$ symmetry) in which the iron sites are occupied by Mn, Ni, and Li and the sodium sites by Li.[23] The detailed structure of the $x = 0.2$ composition has not been described previously; we do so here to provide a starting point for investigating the evolution of structure on lithium extraction. A neutron powder diffraction pattern for our $Li[Ni_{0.2}Li_{0.2}Mn_{0.6}]O_2$ product is shown in Figure 1a. It is known that ordering of the Li/Ni/Mn ions in these nanocomposite structures gives rise to weak superlattice reflections, seen typically between 21 and 25° 2θ in X-ray diffraction (Cu $K\alpha_1$) patterns,[25] which can be indexed in the space groups $C2/m$ or $P3_112$ that characterize the Li_2MnO_3-like components of the structure.[30,32] By using a model in the $C2/m$ space group, an improved fit could be obtained; however, in keeping with previous studies, we have found that no variation in the structural description with regard to Li/Ni site disorder is obtained by using this space group, and instead we have, consistent with previous authors, employed the $R\bar{3}m$ space group for a typical layered structure. The model used for refinement placed Mn/Ni/Li on the octahedral sites in the transition metal layers, whereas both Li and Ni were positioned on the octahedral sites of the lithium layers. Refinement involved fixing the Mn occupancy and varying the ratios of the Ni and Li occupancies on the transition

(25) Kim, J−S.; Johnson, C. S.; Vaughey, J. T.; Thackeray, M. M.; Hackney, S. A.; Yoon, W.; Grey, C. P. *Chem. Mater.* **2004**, *16*, 1996.
(26) Jiang, J.; Eberman, K. W.; Krause, L. J.; Dahn, J. R. *J. Electrochem. Soc.* **2005**, *152*, A1879.
(27) Matthewman, J. C.; Thompson, P.; Brown, P. J. *J. Appl. Crystallogr.* **1982**, *15*, 167.
(28) Sears, V. F. *Neutron News* **1992**, *3*(3), 26.
(29) Ufheil, J.; Baertsch, M. C.; Würsig, A.; Novák, P. *Electrochim. Acta* **2005**, *50*, 1733.
(30) Meng, Y. S.; Ceder, G.; Grey, C. P.; Yoon, W.-S.; Jiang, M.; Bréger, J.; Shao-Horn, Y. *Chem. Mater.* **2005**, *17*, 2386.
(31) Roth, R. S.; Wadsley, A. D. *Acta Crystallogr.* **1965**, *19*, 26.
(32) Lu, Z.; Chen, Z.; Dahn, J. R. *Chem. Mater.* **2003**, *15*, 3214.

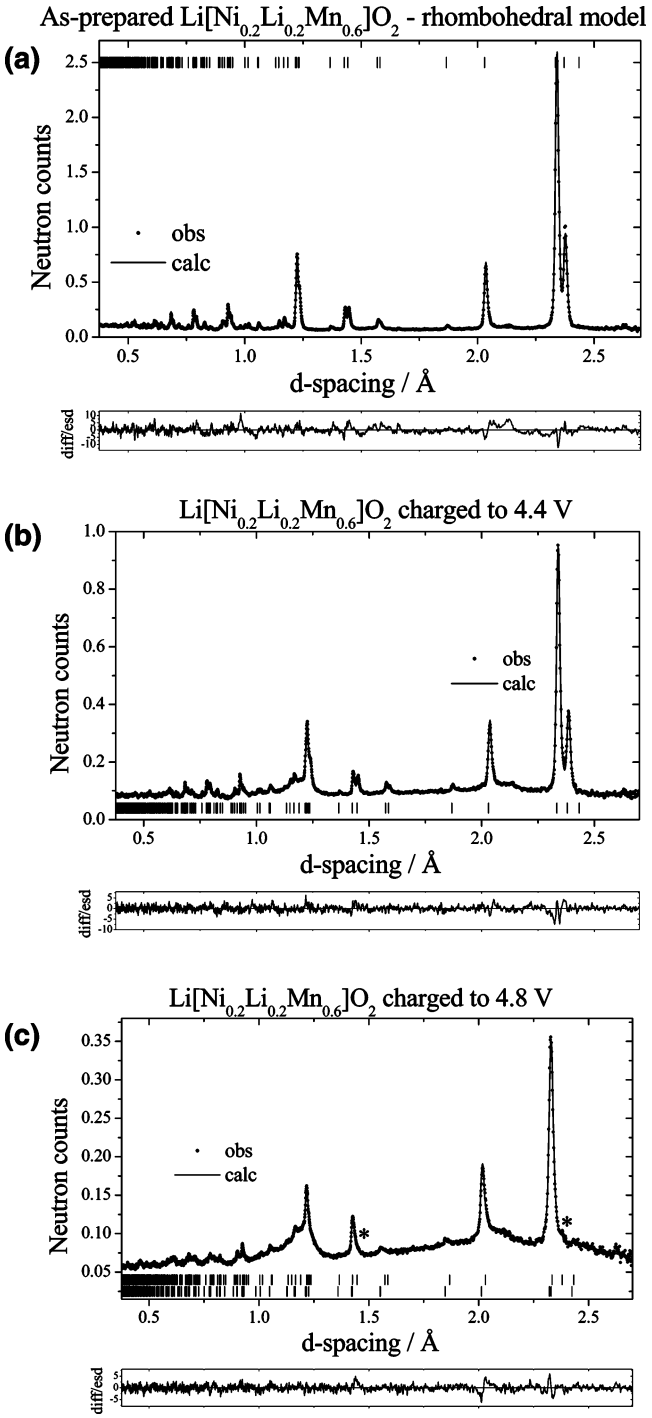

Figure 1. Profile fits for Rietveld refinement of $Li[Ni_{0.2}Li_{0.2}Mn_{0.6}]O_2$. Dots indicate observed data; solid line indicates calculated profile. The lower box shows difference/esd. Tick marks show allowed reflections. (a) As-prepared (single $R\bar{3}m$ phase), (b) charged to 4.4 V, (c) charged to 4.8V, model incorporating two phases (upper tick marks 4.4 V phase, lower tick marks main phase). Some of the major reflections from the 4.4 V phase are marked (*).

metal and lithium sites. A good fit was obtained, Figure 1a, and the refined occupancies yielded an overall stoichiometry of $Li_{1.21}Mn_{0.60}Ni_{0.19}O_2$, in excellent agreement with the anticipated composition, Table 1a.

Previous studies have shown that the degree of Ni/Li exchange between the transition metal and lithium layers increases with increasing x, reaching a value of approximately 10% for $LiNi_{0.5}Mn_{0.5}O_2$ ($x = 0.5$).[23,30,32] For $x = 0.25$ in $Li[Ni_xLi_{1/3-2x/3}Mn_{2/3-x/3}]O_2$, a 3% nickel content of the lithium layers was reported.[32] The displacement of 1.6% Ni into the lithium layers, which is observed in this investigation for $Li[Ni_{0.2}Li_{0.2}Mn_{0.6}]O_2$ ($x = 0.2$), is therefore consistent with the observed trend for this system and also with the reported approach of using intergrown $xLiNi_yMn_{1-y}O_2 \cdot (1-x)Li_2MO_3$ structures in which the layered, lithium-rich Li_2MO_3 component, such as Li_2MnO_3 or Li_2TiO_3, serves to minimize contamination of the lithium layers by transition metal ions.[33]

The variation of potential on extracting lithium from a $Li[Ni_{0.2}Li_{0.2}Mn_{0.6}]O_2$ electrode is shown in Figure 2; the data are in good accord with results for the $Li[Ni_xLi_{1/3-2x/3}Mn_{2/3-x/3}]O_2$ electrode system reported previously.[22−25] Initially, the voltage increases monotonically, corresponding to the oxidation of Ni^{2+} to Ni^{4+}, until a plateau is reached at 4.5 V, at which point all Ni is in the +4 oxidation state.[34−36] Neutron powder diffraction data were collected on an electrode charged to 4.4 V, i.e., within the range of conventional lithium deintercalation. The neutron powder diffraction pattern for this electrode is shown in Figure 1b; as expected, it is similar to that of the as-prepared material. Refinement was carried out using the structural model obtained for the as-prepared phase. With the Mn occupancy fixed, the Ni/Li ratio was varied on the transition metal sites. The nickel content in the lithium layer was held at the value obtained for the as-prepared material, whereas the lithium occupancy was allowed to vary. An excellent fit to the observed profile was obtained ($R_{wP} = 2.92\%$); the refined crystallographic data are presented in Table 1b. The Mn/Ni/Li ratio in the transition metal layer of the "4.4 V phase" is, within experimental error, the same as that in the parent material, Table 1a,b, giving us confidence in the validity of our refinements and indicating that there had been no appreciable lithium extraction from the octahedral sites of the transition metal layers. At 4.4 V, the degree of lithium deintercalation is modest (85 $mAhg^{-1}$), the lithium occupancy in the lithium layers being 0.78(2), which is evidently too high to promote lithium displacement from the transition metal layers. Attempts to identify lithium in tetrahedral sites proved fruitless, in keeping with the high lithium occupancy in the lithium layers.

The voltage plateau at 4.5 V in Figure 2 has been proposed previously to result from the electrochemical removal of Li_2O (lithium extraction and oxygen loss) from the Li_2MnO_3 component of $xLiNi_{0.5}Mn_{0.5}O_2 \cdot (1-x)Li_2MnO_3$ electrode structures.[9] To investigate directly whether the origin of the 4.5 V plateau lies specifically in oxygen loss from our $Li[Ni_{0.2}Li_{0.2}Mn_{0.6}]O_2$ electrode, an in situ mass spectroscopy cell, developed at the Paul Scherrer Institute (PSI) and permitting direct analysis of gases as they are evolved from the electrochemical cell, was employed. During the measurements, a constant stream of argon flows through the headspace of the cell. Gases evolved at the electrode rise within the electrolyte to the headspace where they are pumped off, together with the argon carrier gas, via a capillary to the mass spectrometer. The mass signals were recorded as a function of cell voltage and time. The results

(33) Johnson, C. S.; Kim, J−S.; Kropf, A. J.; Kahaian, A. J.; Vaughey, J. T.; Thackeray, M. M. *Electrochem. Commun.* **2002**, *4*, 492.
(34) Yoon, W.-S.; Paik, Y.; Yang, X.-Q.; Balasubramanian, M.; McBreen, J.; Grey, C. P. *Electrochem. Solid-State Lett.* **2002**, *5*, A263.
(35) Yoon, W.-S.; Grey, C. P.; Balasubramanian, M.; Yang, X.-Q.; McBreen, J. *Chem. Mater.* **2003**, *15*, 3161
(36) Yoon, W.-S.; Balasubramanian, M.; Yang, X.-Q.; Fu, Z.; Fischer, D. A.; McBreen, J. *J. Electrochem. Soc.* **2004**, *151*, A246.

Table 1.

(a) Crystallographic Parameters for As-prepared $Li[Ni_{0.2}Li_{0.2}Mn_{0.6}]O_2$[a]

$R\bar{3}m$. $a = 2.8542(2)$ Å, $c = 14.2253(5)$ Å, $V = 100.361$ Å^3, $Z = 3$, hexagonal setting

atom	Wyckoff symbol	*x*/*a*	*y*/*b*	*z*/*c*	Biso	occupancy
Li1/Ni2	3b	0.0	0.0	0.5	0.92(11)	0.984/0.016(3)
Mn1/Ni1/Li2	3a	0.0	0.0	0.0	0.45(16)	0.6/0.172/0.228(3)
O1	6c	0.0	0.0	0.25847(6)	0.68(2)	1

(b) Crystallographic Parameters for $Li[Ni_{0.2}Li_{0.2}Mn_{0.6}]O_2$ Charged to 4.4V[b]

$R\bar{3}m$. $a = 2.8512(2)$ Å, $c = 14.2793(6)$ Å, $V = 100.526$ Å^3, $Z = 3$, hexagonal setting

atom	Wyckoff symbol	*x*/*a*	*y*/*b*	*z*/*c*	Biso	occupancy
Li1/Ni2	3b	0.0	0.0	0.5	0.75(16)	0.78(2)/0.016
Mn1/Ni1/Li2	3a	0.0	0.0	0.0	0.8(2)	0.6/0.170/0.230(3)
O1	6c	0.0	0.0	0.25963(8)	0.68(2)	1

(c) Crystallographic Parameters for $Li[Ni_{0.2}Li_{0.2}Mn_{0.6}]O_2$ Charged to 4.8V[c] Main phase:[d]

$R\bar{3}m$. $a = 2.843(2)$ Å, $c = 13.954(4)$ Å, $V = 97.651$ Å^3, $Z = 3$, hexagonal setting

atom	Wyckoff symbol	*x*/*a*	*y*/*b*	*z*/*c*	Biso	occupancy
Ni2	3b	0.0	0.0	0.5	0.75(−)	0.019(6)
Mn1/Ni1	3a	0.0	0.0	0.0	0.7(5)	0.778/0.222(5)
O1	6c	0.0	0.0	0.25864(19)	1.17(5)	1

[a] R-factors: $R_{exp} = 2.45\%$, $R_{wP} = 5.58\%$, $R_P = 4.64\%$. [b] R-factors: $R_{exp} = 2.22\%$, $R_{wP} = 2.92\%$, $R_P = 2.57\%$. [c] R-factors: $R_{exp} = 1.83\%$, $R_{wP} = 2.26\%$, $R_P = 2.01\%$. [d] Phase ratio 0.897/0.103(7).

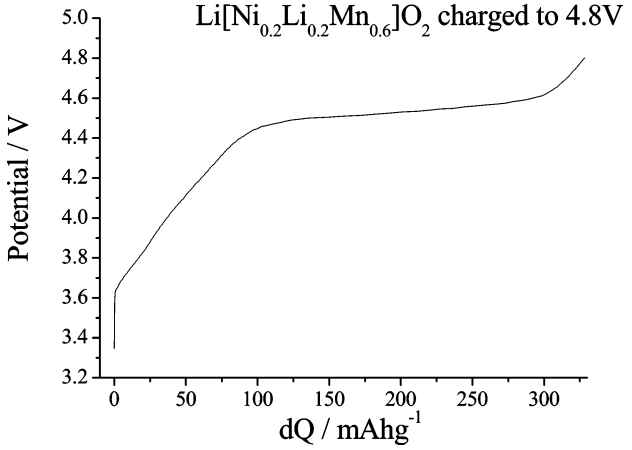

Figure 2. Variation of potential (vs Li^+[1 M]/Li) with state of charge for $Li[Ni_{0.2}Li_{0.2}Mn_{0.6}]O_2$ at a rate of 10 mAg^{1-}.

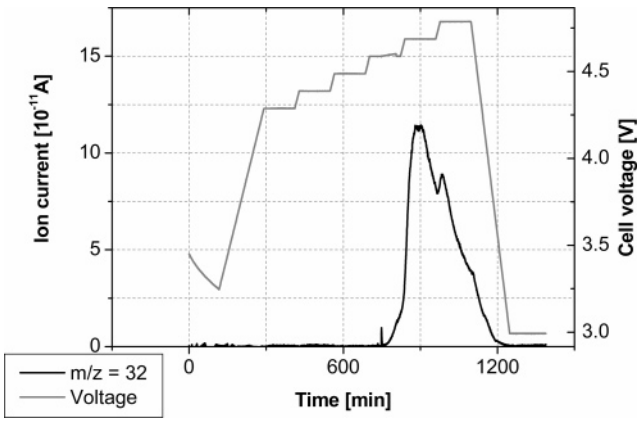

Figure 3. Ion current vs charging time and cell potential from the mass spectrometry analysis of O_2 evolved on charging $Li[Ni_{0.2}Li_{0.2}Mn_{0.6}]O_2$.

obtained on charging the $Li[Ni_{0.2}Li_{0.2}Mn_{0.6}]O_2$ electrode in steps of 0.1 V, from 4.3 V with 120 min spent at each voltage, are reported in Figure 3. Evolution of oxygen was observed, which became important from potentials above 4.5 V, corresponding to the plateau in Figure 2. Similar results were obtained with different electrolytes. The next most abundant gas was CO_2, coming from a side reaction implying partial oxidation of the electrolyte. Such CO_2 evolution due to electrolyte decomposition has been reported previously.[29] Although we cannot determine the absolute quantities of the gases evolved, CO_2 evolution was estimated to be less than 10% of the O_2 evolution. These results provide direct evidence of oxygen evolution associated with the 4.5 V plateau.

To consider the structural rearrangements that accompany oxygen evolution, we collected neutron powder diffraction data for a $Li[Ni_{0.2}Li_{0.2}Mn_{0.6}]O_2$ electrode after charging across the 4.5 V plateau, to 4.8 V (Figure 1c). Despite a small amount of residual "4.4 V phase" in the neutron data, it is immediately apparent that the loss of oxygen during the two-phase reaction at 4.5 V causes significant structural changes to the electrode.

Although it is acknowledged that some oxygen evolution may occur accompanied by the highly oxidizing Ni^{4+} ions being reduced to Ni^{3+} or even Ni^{2+} at the surface of charged electrode particles, as has been observed in lithium-depleted $Li_{1-x}Ni_{0.8}Co_{0.2}O_2$ electrodes,[37] the electrochemical data obtained from $Li[Ni_xLi_{1/3-2x/3}Mn_{2/3-x/3}]O_2$ electrodes necessarily imply that another mechanism for oxygen loss must occur to account for the extraordinarily high capacities (220−250 mAh/g) delivered by these electrodes.[22,24] From a structural viewpoint, two models are considered to explain the oxygen loss phenomenon. As Li and O leave the surface of the charged $Li[Ni_{0.2}Li_{0.2}Mn_{0.6}]O_2$ electrode particles, oxide ions could diffuse from the bulk to the surface, thus sustaining the reaction. This would involve the creation of O^{2-} vacancies within the electrode structure. All attempts to refine a model based on the introduction of O^{2-}

(37) Abraham, D. P.; Twesten, R. D.; Balasubramanian, M.; Kropf, A. J.; Fischer, D.; McBreen, J.; Petrov, I.; Amine, K. *J. Electrochem. Soc.* **2003**, *150*, A1450.

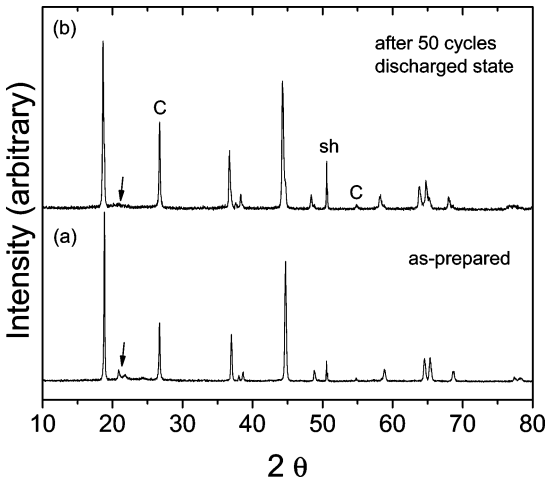

Figure 4. X-ray diffraction patterns of (a) as-prepared $Li[Ni_{0.2}Li_{0.2}Mn_{0.6}]O_2$ and (b) after 50 charge/discharge cycles in a lithium cell between 4.6 and 2.0 V (discharged state). C and sh denote carbon additive in the electrode and X-ray sample holder, respectively.

vacancies failed, yielding oxygen occupancies that were greater than unity (1.35). Consideration was, therefore, given to a second model in which oxygen loss from the surface is accompanied by transition metal ions diffusing from the surface into the bulk and entering the octahedral sites vacated by Li^+ ions as the latter are extracted from octahedral sites in the transition metal layers. Note that for the cycled $Li[Ni_{0.2}Li_{0.2}Mn_{0.6}]O_2$ electrode, the weak superlattice reflections disappear (expected peak positions arrowed in Figure 4), consistent with the removal of lithium from the transition metal layers, associated loss of Li/Mn/Ni order, and a condensation of manganese and nickel in the octahedral sites left vacant by the lithium ions.

On the basis of the amount of charge passed (328 mAh/g), and taking into account the proportion of the residual "4.4 V phase" in the electrode at 4.8 V (10%) obtained from the two-phase refinement, we calculate that, at 4.8 V, 1.13 lithium ions (i.e., 94% of the initial content) had been extracted from the major phase. Of these ions, 0.40 were associated with the oxidation of Ni^{2+} to Ni^{4+}, with the balance of 0.73 associated with oxygen loss (oxidation of lattice O^{2-} ions), corresponding to a reduction of 0.365 in the oxygen content of the electrode. Using the manganese and nickel contents in the refined "4.4 V phase" and taking into account the oxygen loss during charge, the formula for the "4.8 V phase" is determined to be $(Li_{0.07}Ni_{0.016})[Mn_{0.6}Ni_{0.17}]O_{1.64}$. When normalized to a fully close-packed oxygen lattice (i.e., without any oxygen vacancies) and assuming that the residual lithium ions reside in the lithium layers rather than in the transition metal layers, the formula is $(Li_{0.09}Ni_{0.019})[Mn_{0.73}Ni_{0.21}]O_2$, in which the sum of the Mn and Ni octahedral-site occupancy in the transition metal layers is close to unity (0.94); As a result, we use a layered ($R\bar{3}m$) structure as a starting model for the refinement of the "4.8 V phase", in which the octahedral transition metal sites are fully occupied by Mn and Ni and in which the octahedral sites in the lithium layer are occupied by a small amount of Ni (0.016). Although there are certainly some residual lithium ions in the "4.8 V phase", the amount is small (0.09); introducing this minor amount of lithium into either the transition metal- or lithium-layer sites makes only a marginal difference to the nickel occupancies—and insignificant changes to the *R* factors (Li scattering length $= -0.19 \times 10^{-12}$ cm and Ni $= +1.03 \times 10^{-12}$ cm). As a result, we omitted lithium from the final refinements. In these refinements, the Mn/Ni ratio in the transition metal sites and the Ni occupancy in the lithium layers were varied. Such a model provided an excellent fit between the experimental and calculated data ($R_{wP} = 2.26$), and it confirmed, within experimental error, that the Mn-to-Ni ratio (3.5:1) in the transition metal layers and the nickel content in the lithium layers (0.019(6)) had remained essentially unchanged during the activation process from 4.4 to 4.8 V. Moreover, the refined manganese and nickel occupancies in the transition metal layers of the "4.8 V phase", reported in Table 1c, support the argument that, on electrochemical activation, there is a condensation of manganese and nickel in the octahedral sites of the transition metal layers left vacant by lithium as it diffuses out from these layers and oxygen is removed from the structure at and above 4.5 V.

Conclusion

In conclusion, we have presented direct evidence for oxygen evolution associated with charging a layered lithium−manganese−nickel−oxide electrode with Li_2MnO_3-like character beyond the typical limit for deintercalation, usually ~4.2 V. Combining this information with our structural data, the mechanism for oxygen loss in such materials may be summarized as follows. Beyond the conventional intercalation limit, at 4.5 V, the Fermi level will be situated within the oxygen valence band. Electron removal from O^{2-} species at the surface will, therefore, accompany Li^+ extraction. As oxygen is evolved from the surface, lithium ions migrate from the octahedral sites in the transition metal layers into the lithium layers leaving vacancies, which are subsequently occupied through a cooperative displacement of the transition metal ions diffusing from the surface into the bulk, something that continues until all the octahedral sites vacated by the lithium ions are occupied by transition metals, at which point oxygen evolution ceases. The net effect of charging across the 4.5 V plateau is the removal of Li_2O from the electrode structure, which results in a layered MO_2 electrode structure in which the M octahedral sites are occupied almost exclusively by manganese and nickel. It is this material which then acts as a host structure for reversible lithium intercalation/deintercalation and gives rise to reversible capacities in excess of 200 $mAhg^{-1}$.[24]

Acknowledgment. P.G.B. acknowledges support from the Royal Society, The EPSRC, and European Union. M.M.T., C.S.J., and S.-H.K. gratefully acknowledge support from the Office of FreedomCar and Vehicle Technologies (Batteries for Advanced Transportation Technologies (BATT) Program) of the U.S. Department of Energy. We also acknowledge Andreas Würsig and Werner Scheifele for their contribution to the development of the DEMS method.

JA062027+